12-22-2021

Realistic Additions to MATLAB Simulation of Active Particles in an Acoustic Field

Emily Ma
Washington University in St. Louis

Realistic Additions to MATLAB Simulation of Active Particles in an Acoustic Field

Emily Ma

Introduction

Acoustic microfluidics provides a contact-free method of manipulating active particles; however, versatile and quick performance quantification of these methods is needed to further apply acoustofluidic techniques in broader settings. Motile *Chlamydomonas reinhardtii* algae cells continuously swim and redistribute as they are subject to an acoustic field. For performance quantification, this eliminates the tedious procedure of resetting the experiment after each trial, which is necessary when using passive particles as probes. Thus, this method of calibration using active particles is more efficient than using passive particles. Utilizing an accurate simulation of physical active particle experiments is helpful in quickly predicting how changes in individual variables will affect the particle distribution; to know that the experiment is being done correctly, physical experimentation results should follow the simulation results. An existing mathematical simulation that models the behavior of active particles in a known acoustic field within the confines of a given channel was improved to be more realistic. Having an accurate simulation would allow large numbers of simulations under various conditions to be run quickly, saving time and resources. This MATLAB model initially contained arbitrary swimming biases that were an idealized version of swimming cell behavior; the movement and resulting distribution of the cells within an acoustic field were not accurate to physical experiments. Various forces, randomizations, and biases were implemented to observe their effect on cell distribution. Further work would be spent on comparing the simulated particle distribution within an acoustic field to experimental data and making further adjustments to the MATLAB script from there. Further, lubrication forces or particle-particle interactions involving the cells could be added.

Methods

The primary programming language used for making changes to the acoustic field simulation was MATLAB. The initial simulation imposed heavy restrictions on the reorientation abilities of the cells. This was a 3D simulation with a channel length, width, and height of 834 micrometers, 375 micrometers, and 49 micrometers, respectively. The simulated liquid within the channel was water with a density of 997 kg/m^3; the compressibility and viscosity of the water were also given. Particle properties, including density, compressibility, radius, and swimming speed were taken from Minji Kim's physical experimentation, and these values, along with their associated uncertainties, were input to the simulation [1]. The angle reorientation is based on spherical coordinates, with an azimuth angle (phi) range from 0 to 2π and an altitude angle (theta) range from 0 to π. An arbitrary swimming restriction was used in the initial model, leading to cell movement that was unrealistic. Cells were restricted to moving along the channel width with minimal movement along the length of the channel.

Most of the changes made to the simulation between trials regarded the number of particles generated within the channel, the energy density, and the observation time increment. The distribution of the cells along the channel width (Y direction) is plotted in a histogram using

150 bins. The initial coordinate location and swimming angle of the cells are randomized when the cells are initially loaded into the channel. All the cells in the trap have the same velocity and reorientation time, but they have a randomized uncertainty associated with both values.

The random restriction was removed from the received MATLAB code. The cells were now given the full sphere of angles to reorient into for random reorientations. If the cells encountered any of the walls of the channel, the possible reorientation was the hemisphere away from the wall. This prevented the cell from continuously reorienting directly into the wall of the channel. However, removing the bias resulted in a histogram distribution of the cells for the last 3 seconds that no longer represented a two-peak distribution, like in physical experiments (Fig. A).

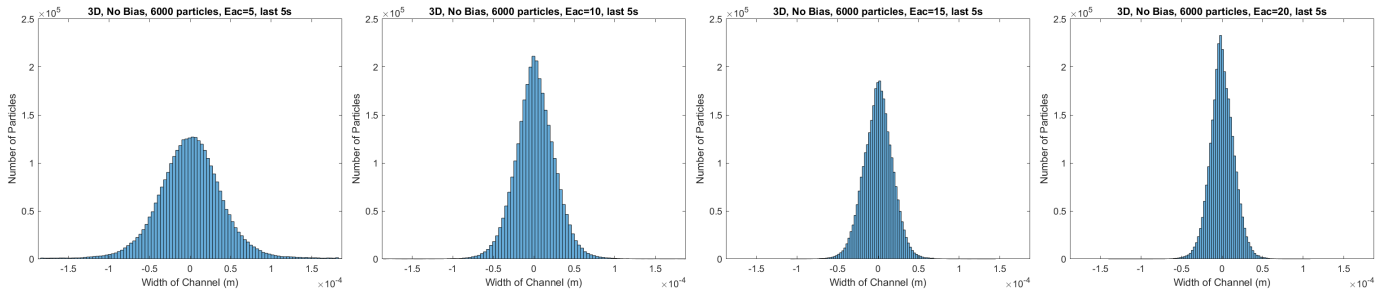

Figure A: Histogram plot of cell distribution along channel width for 3D simulation

It was clear that a bias was necessary to have the simulation match the real-life experimentation. Many random factors are difficult to represent with mathematical equations, so the 3D model was first simplified, and 2D simulations were observed to see how various added biases would affect the cell distribution along the channel width.

1D Simulation

First, the simulation was further simplified from a two-dimensional plane to a one-dimensional line to determine if the two-peak distribution remained consistent. Particles were initially randomly distributed along this line. When an acoustic field is applied, the particles can only move in the negative and positive Y directions. The particles only have two possible directions of random reorientation. There are no X and Z direction boundary conditions to check for; there are only boundary checks at the width of the channel. These conditions were checked with 6,000 particles at a variety of acoustic energy densities. There was a very significant and clear two-peak distribution at each energy density. Histograms created using this 1D simulation with various energy densities are shown in Fig. B.

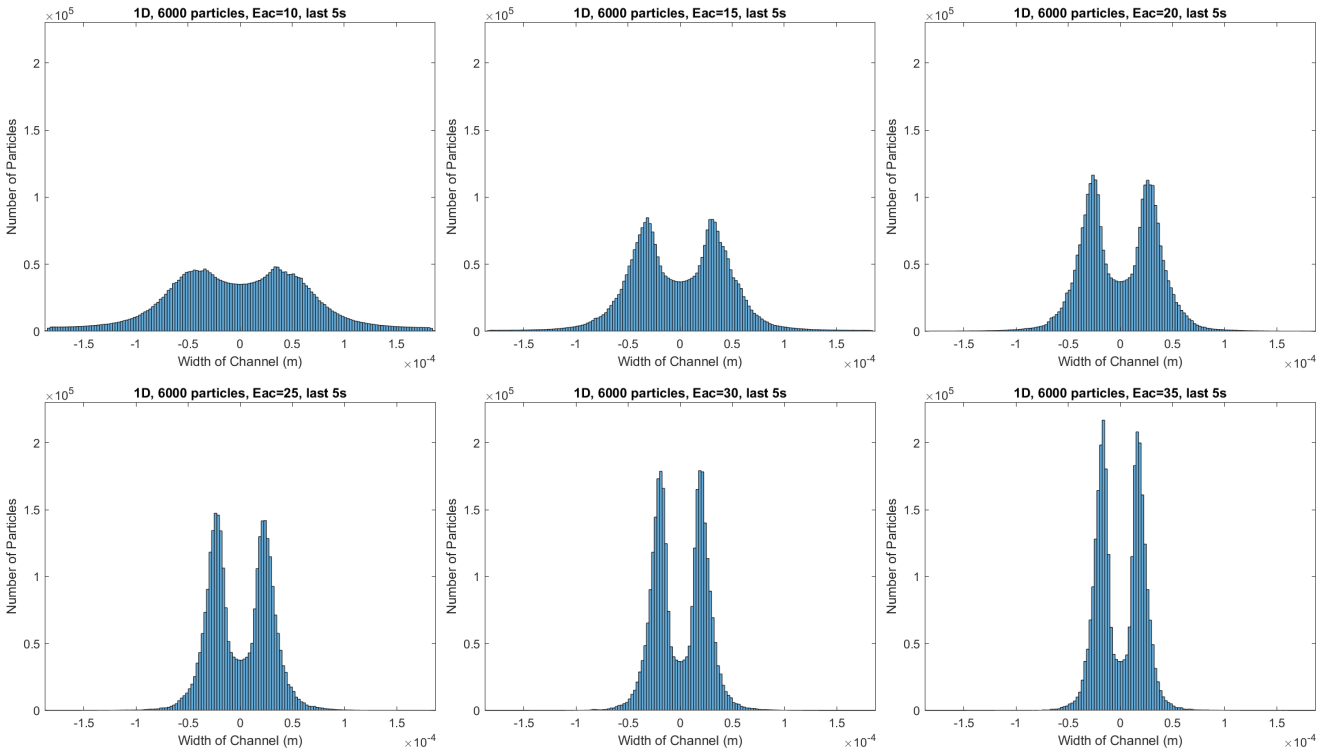

Figure B: Histogram plot of cell distribution along channel width for 1D simulation at various acoustic energy densities

These peaks are much larger than the 2D simulations, indicating that the cells are much more confined within the two potential minima within the 1D "channel". It makes sense that these peaks are much larger than real experimentation results. The particles do not traverse along the length of the channel, and they are therefore trapped at the minima much more quickly.

2D Simulations

Simplified 2D plane section views were also observed to see how their distribution differed from the 3D single-peak distribution. Observing the YZ plane only involved theta as a random reorientation angle ranging from 0 to 2π. The XY plane involved the random reorientation angle of phi of the same range, but otherwise, the section cuts initially operated similarly. Several trials of this 2D XY plane at varying energy densities are shown below in Fig. C.

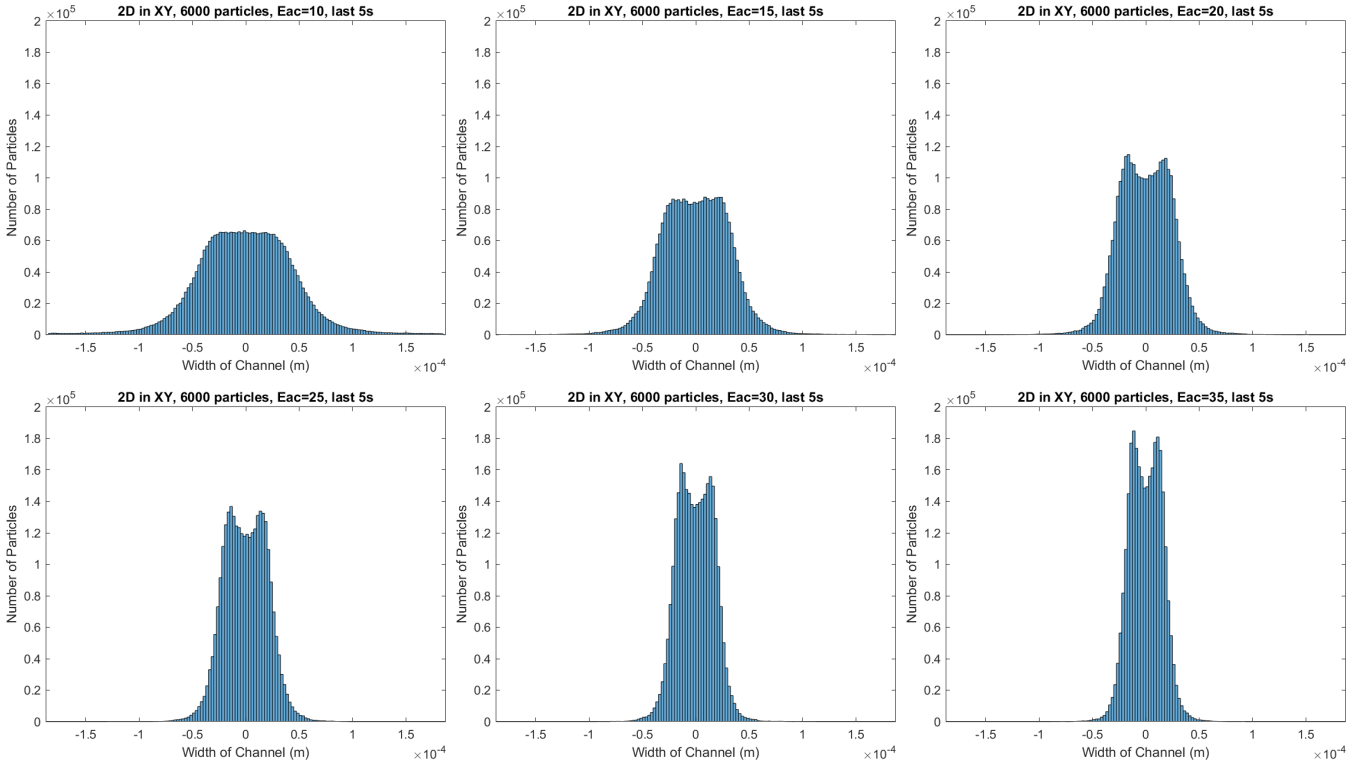

Figure C: Histogram plot of cell distribution along channel width for 2D XY plane simulation at various energy densities

In experimentation, the swimming cells have a bias for swimming parallel to the top and bottom of the channel. This is due to several reasons. The *C. reinhardtii* cells have two cilia that extend around 11.6 micrometers from their body [2]. When one of the cilia touches a wall, the swimming cell senses it and may reorient away from the wall before the cell body senses the wall. As the height of the channel is only 49 micrometers, this detection through cilia is much more likely at the top and bottom of the channel. The lubrication forces from the walls are also stronger due to the top and bottom walls; this makes it easier for the cells to swim along the length of the channel, as they do not need to overcome the lubrication forces due to the squeezing motion of the fluid through the gap between the cell and the wall [1].

Two strategies to correctly simulate the cells' YZ swimming direction bias were implemented. The first of which designated an "angle cone" that the cell was allowed to reorient into, rather than the full 2π radians. As an example, the cells were first tested under a restrictive reorientation angle cone of $\pi/4$; if a cell was traveling in the positive Y direction, at the center of the channel, the cell could reorient randomly in the $-\pi/8$ to $\pi/8$ range. As the cell traveling in the positive Y direction approached the top or bottom wall of the channel, this possible $\pi/4$ cone shifted so the wall was one of the range boundaries; if the cell needed to randomly reorient at the very bottom of the channel, the angle range was from 0 to $\pi/4$ radians. A corresponding bias was set if the cell was traveling left. Even if the reorientation "angle cone" was designated to be larger than $\pi/4$, this bias method was deemed to be over-restrictive as the cell could not change its Y direction of movement once it was given an initial velocity.

When taking YZ section cuts of the channel, both the azimuthal and altitude angle must be taken into consideration. The reorientation range of the altitude angle is 0 to π, like in the original 3D simulation; this angle is defined as 0 indicating the particle is traveling straight up and π indicating the particle is traveling straight down. There are only two possible options for the azimuthal angle, which controls whether the particle is moving in the positive or negative Y direction. The particle traveling in the positive Y-direction if π/2 and traveling in the negative Y-direction if 3π/2.

The second method involved a more lenient restriction where the cell could randomly reorient into the full 2π range in the very center of the channel. The sections that were cut out of the possible reorientation circle scaled linearly from the middle of the channel to the top and bottom walls. The resulting histograms from this method are shown in Fig. D. At the top of the channel, the possible random reorientation angle ranges from π/2 to π for the altitude angle and π/2 or 3π/2 for the azimuthal angle. At the bottom of the channel, the possible random reorientation angle ranges from 0 to π/2 for the altitude angle and π/2 or 3π/2 for the azimuthal angle.

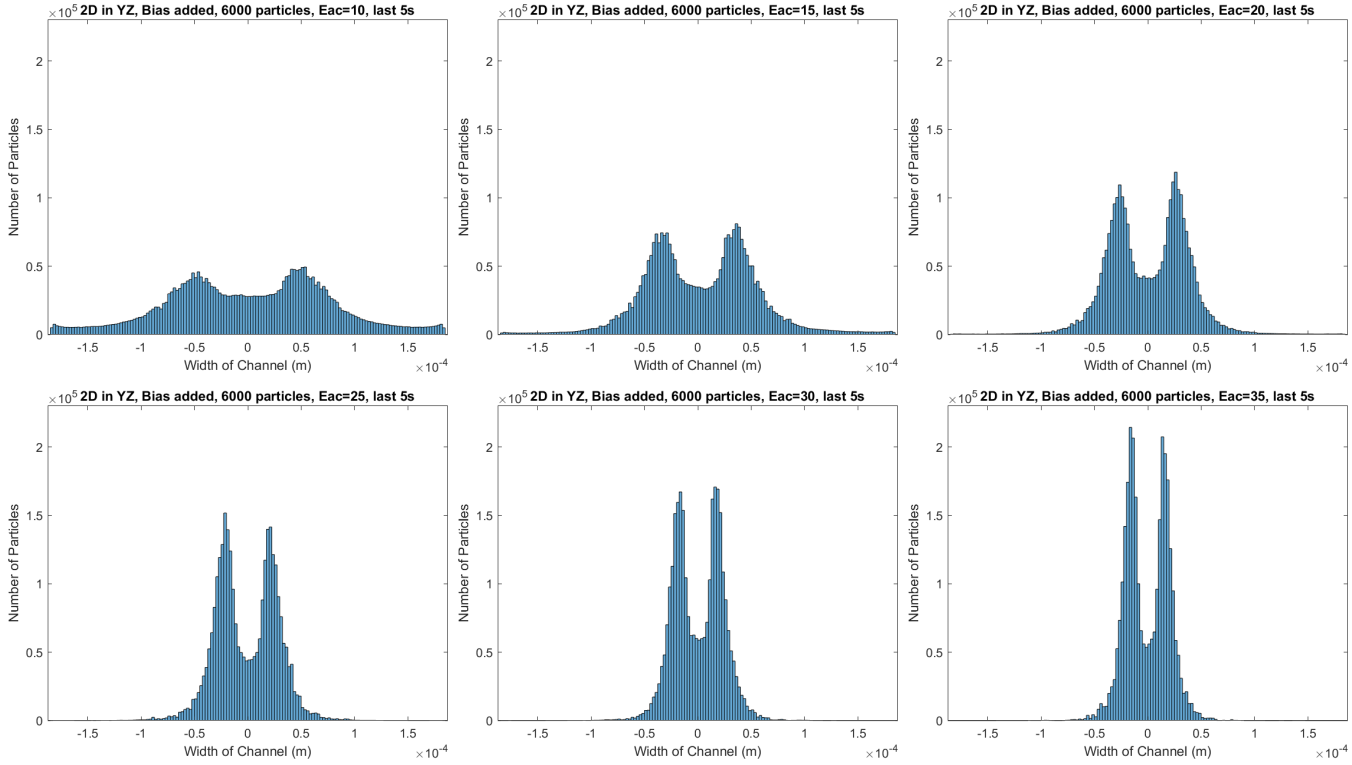

Figure D: Histogram plot of cell distribution along channel width for 2D YZ simulation with added bias at various energy densities

3D Simulation

The second method of angle bias was added back to the 3D simulation; the cells now preferentially swam parallel to the length of the channel when exposed to an acoustic field. The

resulting histograms in Fig. E show less of a uniform one-peak distribution than the previous histograms with no biases.

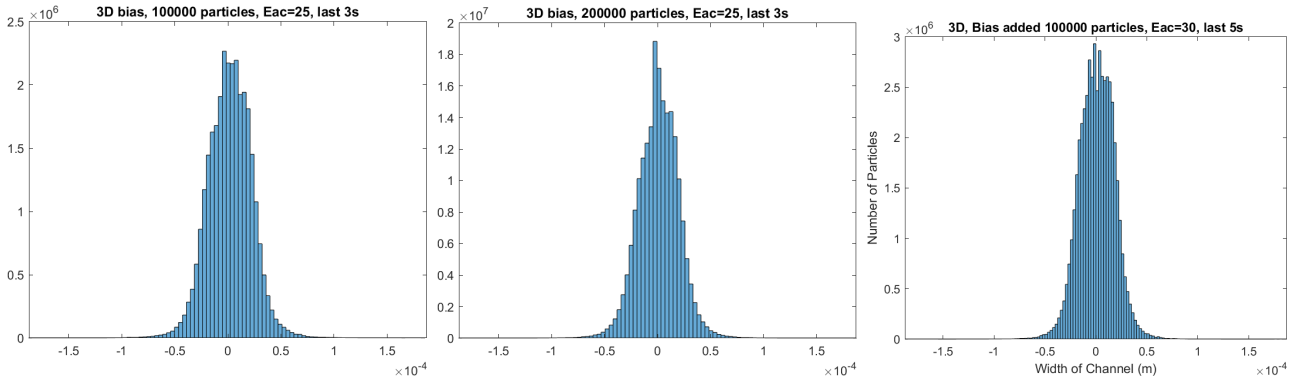

Figure E: Histogram plots of cell distribution along channel width for 3D simulation with added bias at various energy densities

Results and Discussion

Initially, the model's only concern was the primary acoustic radiation force and the intrinsic swimming capabilities of the cells. More complicated forces, namely the wall interaction and their effects on the swimming cells, were added to the model to better simulate real behavior. Simulations with different experimental procedures were modeled, including trials subject to different channel architecture, acoustic field strength, and the number of cells within the channel.

These additions were applied to the 3D model, but the plots in Figure E are not as symmetric as would be expected for trials with such large numbers of particles. It appears that the particles still have not reached a steady-state distribution. "the distributions showed less of a uniform Gaussian distribution, though they also appear to have a slight asymmetry, which is not expected based on the mathematical equations that describe the system. Future work should focus on identifying the source of this asymmetry within the model. Adding valid and variable lubrication forces and secondary acoustic radiation forces would further aid in the accuracy of this model. This was more difficult than expected as the randomized movement of cells is difficult to represent with mathematical equations without thorough experimentation. Direct comparisons to histograms generated from real-life experimentations could confirm the current findings regarding the cell swimming biases, and further adjustments can be made to the restrictions.

Future work on the model would include lubrication forces and secondary acoustic radiation forces due to scattering. Currently, the cells are represented as single-point particles, each having a velocity and reorientation time; code could be added that represents cell-to-cell interactions within the channel. There are no cell-to-cell interactions within the model. However, the lack of forces does not discount the work done on the simulation; the cell-to-cell interactions are expected to have a smaller effect on the resulting cell distribution along the channel width.

Conclusion

The work done in this study is the first step to developing an accurate active particle model in an acoustic field. Wall interaction forces have been thoroughly investigated, and there is a solid foundation to build upon for adding other forces, including lubrication forces between cells and secondary radiation forces. Future work could also involve comparing the simulation histogram results to physical experimentation under similar channel architecture, energy density, and particle count. Further modifications to the wall interaction forces will have to be made through trial and error as it is difficult to represent the behavior of random cells with simple math equations. The simulation follows the real behavior of *C. reinhardtii* cells more closely than at the start of this study.

Literature Cited

[1] Kim, Minji, Barnkob, Rune and Meacham, J. Mark. “Rapid measurement of the local pressure amplitude in microchannel acoustophoresis using motile cells.” *The Journal of the Acoustical Society of America* Vol. 150 No. 1565-1576 (2021). DOI https://doi.org/10.1121/10.0005910.

[2] Huddleston, Joanna. “Rulers and sensors in Chlamydomonas.” *Nature Reviews Microbiology* Vol. 9 No. 397 (2011). DOI https://doi.org/10.1038/nrmicro2584.